

Synthesis and Structure–Activity Relationship for a Novel Class of Potent and Selective Carbamate-Based Inhibitors of Hormone Selective Lipase with Acute In Vivo Antilipolytic Effects

Søren Ebdrup,* Hanne Hoffmann Frølund Refsgaard, Christian Fledelius, and Poul Jacobsen

Novo Nordisk A/S, Novo Nordisk Park, 2760 Måløv, Denmark

Received June 28, 2006

Hormone-sensitive lipase (HSL) is an intracellular enzyme that has a central role in the regulation of fatty acid metabolism. The enzyme, therefore, is a potentially interesting pharmacological target for the treatment of insulin resistance and dyslipidemic disorders. Based on a high throughput screening, a carbamate based HSL inhibitor was identified and optimized into the selective HSL inhibitors 4-hydroxymethyl-piperidine-1-carboxylic acid 4-(5-trifluoromethylpyridin-2-yloxy)-phenyl ester (**13f**) and 4-hydroxy-piperidine-1-carboxylic acid 4-(5-trifluoromethylpyridin-2-yloxy)-phenyl ester (**13g**), with IC₅₀ values of 110 and 500 nM, respectively. Both inhibitors were active in acute antilipolytic experiments in vivo and none of the inhibitors inhibited the cytochrome P450 (CYP) isoforms 2D6, 3A4, and 1A2.

Introduction

The causes of type 2 diabetes, including the metabolic syndrome, are complex and involve both genetic and acquired factors.¹ Among the acquired defects, lipotoxicity,² glucotoxicity,³ and obesity⁴ all have been shown to exacerbate insulin resistance and contribute to the decline in β -cell function.

Increased levels of plasma and tissue fatty acids and triglycerides are often present in patients with type 2 diabetes.⁵ The elevated level of plasma fatty acids (FA) are thought to play a major role in the pathogenesis of insulin resistance and type 2 diabetes^{6–8} by inhibiting glucose uptake and utilization by muscle^{9,10} and causing increased glucose output by the liver.^{11–13} These events combine to give the hyperglycemia that is characteristic of type 2 diabetes.¹⁴ Moreover, elevated triglycerides, insulin resistance, and hyperinsulinemia, cardinal characteristics of type 2 diabetes, may be involved in the development of cardiovascular disease in type 2 diabetic patients.¹⁵

Triglycerides are a major source of stored energy. Energy is released from these lipids by hydrolysis followed by oxidation, primarily β -oxidation, of the liberated FA during periods of low-energy intake. Regulation of the synthesis and mobilization of triglycerides is, therefore, essential for energy homeostasis. Most of the increase in plasma FA levels seen in type 2 diabetic patients is the result of increased nocturnal and postprandial adipose tissue lipolysis.¹⁶ Hormone-sensitive lipase (HSL) is thought to be the rate-limiting enzyme in adipose tissue lipolysis and net FA mobilization.¹⁷ The activity of HSL is acutely activated via cAMP and protein kinase A mediated phosphorylation¹⁸ and its regulation in adipocytes is the primary means by which lipolytic agents, such as adrenalin/noradrenalin, control the circulating levels of FA. During periods of high-energy intake, insulin stimulation of adipocytes prevents HSL activation, leading to a decrease in the release of FA and glycerol.¹⁹ The pivotal role of elevated plasma FA in the development of insulin resistance and type 2 diabetes has led to the proposal that HSL may be a potential therapeutic target for this disease, lowering plasma FA levels and, thereby, reducing insulin resistance. However, the nonobese phenotype of HSL knock-

out mice^{20,21} and the accumulation of diglycerides, not triglycerides, in their adipose tissue²² suggest that there may be another lipase involved in the regulation of lipid storage and mobilization. Thus, it has been suggested that although HSL catalyzes the rate-limiting step in triglyceride hydrolysis and is able to hydrolyze both tri- and diglycerides, the major physiological substrate for this enzyme is diglyceride. The recently identified adipose triglyceride lipase (ATGL), is suggested to hydrolyze triglycerides to generate diglycerides that are then further hydrolyzed by HSL.²³ Selective HSL inhibitors may provide useful tools to further clarify the role of HSL and ATGL in lipolysis.

During the last couple of years, a range of different classes of HSL inhibitors have been described by different companies. Bayer has published work on 2*H*-isoxazol-5-ones (**1**),²⁴ Aventis has published work on oxadiazolones (**2**),^{25,26} Ontogene has published work on pyrrolopyrazinediones (**3**),²⁷ and Novo Nordisk has published work on carbazates (**4**),²⁸ carbamoyl-triazoles (**5**),²⁹ and aryl boronic acids (**6**; Figure 1).³⁰ In this paper, a lead optimization program for a range of carbamate-

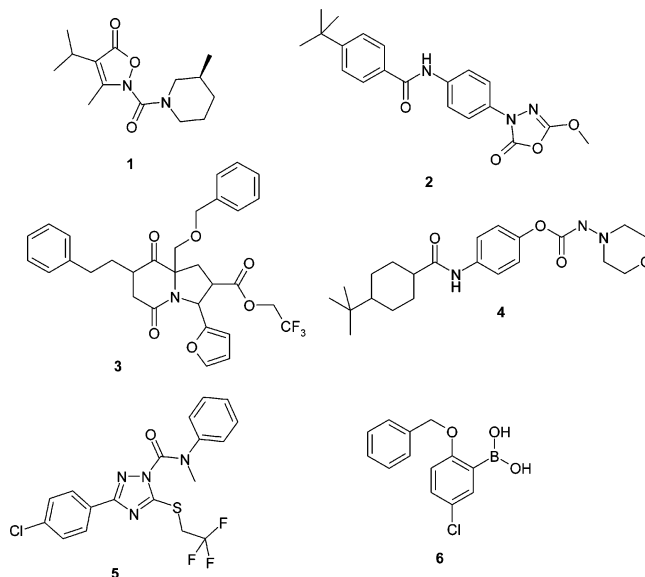


Figure 1. Chemical structures of related HSL inhibitors.

* To whom correspondence should be addressed. Phone: + 45 46752549. Fax: + 45 39179714. E-mail: sebdrup@yahoo.dk.

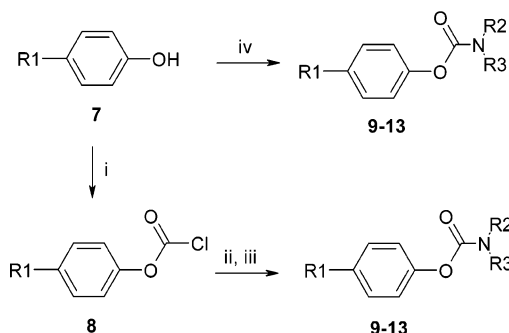


Figure 2. Synthetic route for carbamates. (i) Diphosgene, DIPEA, $\text{CH}_2\text{-Cl}_2$; (ii) amine:



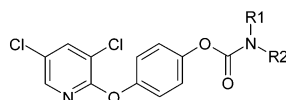
THF, or DCM; (iii) DABCO, carbamoyl chloride, THF; (iv) 1-methyl-3*H*-imidazol-1-ium iodide, acetonitrile.

based HSL inhibitors found in high-throughput screening is presented together with acute rat in vivo data.

Chemistry

The compounds synthesized were independently prepared by three different synthetic methods as described below and in the Experimental Section. Different phenols (**7**) were converted to different chloroformates (**8**) with phosgene or triphosgene. The respective chloroformates were converted to different carbamates (**9–13**). The respective phenols are for some cases also converted to carbamates (**9–13**) via a reaction with a 1-methyl-3*H*-imidazol-1-ium iodide or a carbamoyl chloride as shown in Figure 2. The yields, preparation, and purification methods are given in Tables 1–5. The ^1H and ^{13}C NMR data show that a range of compounds exist as isomers due to hindered rotation around the carbamate group. The isomers cannot be resolved by liquid chromatography.

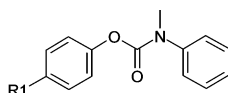
Table 1. Enzyme Activity and Selectivity for 2-Alkoxy-3,5-dichloropyridine-Based HSL Inhibitors



No	Molecule	HSL IC ₅₀ (μM)	AChE IC ₅₀ (μM)	BChE IC ₅₀ (μM)	Preparation Method	Purification	Yield/%
9a		0.35	>50	19			
9b		>50	>50	>50	1 ^a	Chromatography EtOAc/heptane (1:4 → 1:3)	95
9c		3.1	>50	>50	1 ^b	Prep. HPLC	45
9d		0.63	>50	>50	1 ^c	Chromatography EtOAc/heptane (1:6)	81
9e		3.9 ± 0.10 ^d	>50	>50	1 ^e	Prep. HPLC	64

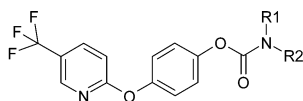
^a *N,N*-Dimethylcarbamoyl chloride. ^b 4-Morpholinylcarbamoyl chloride. ^c *N*-Methyl-*N*-phenylcarbamoyl chloride. ^d IC₅₀ ± SEM ($n = 2$). ^e 1-Pyrrolidinylcarbamoyl chloride.

Table 2. Enzyme Activity and Selectivity for Methyl-phenyl Carbamates-Based HSL Inhibitors



No	Molecule	HSL IC ₅₀ (μM)	AChE IC ₅₀ (μM)	BChE IC ₅₀ (μM)	Preparation Method ^a	Purification	Yield/%
9d		0.63	>50	>50	-	-	-
10a		> 5	>50	>50	1	Recrystallized (EtOH/H ₂ O)	86
10b		8.5	>50	>50	1	Prep. HPLC	41
10c		0.35	>50	>50	1	Recrystallized (EtOH/H ₂ O)	78
10d		0.046 ± 0.015 ^b	>50	>50	1	Chromatography (EtOAc/heptane 1:5)	81
10e		0.046 ± 0.019 ^c	>50	>50	1	Recrystallized (EtOH)	46
10f		1.23	>50	>50	1	Prep. HPLC	32

^a *N*-Methyl-*N*-phenylcarbamoyl chloride. ^b IC₅₀ ± SEM ($n = 2$). ^c IC₅₀ ± SEM ($n = 5$).

Table 3. Enzyme Activity and Selectivity for 2-alkoxy-5-trifluoromethyl Based HSL Inhibitors

No	Amine/ 	HSL IC ₅₀ (μ M)	AChE IC ₅₀ (μ M)	BChE IC ₅₀ (μ M)	Preparation Method	Purification	Yield/ %
11a		> 5	>50	>50	2 ^{a,b}	Chromatography EtOAc/heptane (1:5)	77
11b		> 5	>50	>50	2 ^{a,c}	Prep. HPLC	34
11c		> 5	>50	>50	2 ^{a,d}	Chromatography EtOAc/heptane (1:5)	80
11d		1.4	>50	>50	2 ^{a,e}	Chromatography EtOAc/heptane (1:5)	69
10e		0.046 \pm 0.019 ^f	>50	>50	-	-	-
11e		>5	>50	>50	2 ^{a,g}	Chromatography EtOAc/heptane (1:5)	78
11f		0.023	>50	>50	3	Chromatography EtOAc/heptane (1:4)	93
11g		3.2	>50	>50	2 ^{h,i}	Recrystallized, EtOH	90
11h		> 5	>50	>50	2 ^{a,j}	Chromatography EtOAc/heptane (1:5)	73
11i		0.25	>50	>50	1 ^k	Recrystallized, EtOH	50
11j		0.68	>50	>50	2 ^{a,l}	Prep. HPLC	39
11k		0.065 \pm 0.016 ^m	>50	8.2	2 ^{n,o}	Recrystallized, EtOH	75
11l		1.1	>50	> 50	2 ^{a,b}	Recrystallized, EtOH	53
11m		> 5	>50	>50	2 ^{c,d}	Prep. HPLC	66

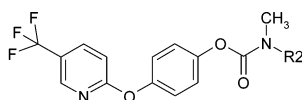
^a Reflux 18 h. ^b 3-(Isopropyl-methyl-carbamoyl)-1-methyl-3H-imidazol-1-ium; iodide. ^c 3-(*tert*-Butyl-methyl-carbamoyl)-1-methyl-3H-imidazol-1-ium; iodide. ^d 3-(Cyclohexyl-methyl-carbamoyl)-1-methyl-3H-imidazol-1-ium; iodide. ^e 3-(Benzyl-methyl-carbamoyl)-1-methyl-3H-imidazol-1-ium; iodide. ^f IC₅₀ \pm SEM ($n = 2$). ^g 3-(Ethyl-phenyl-carbamoyl)-1-methyl-3H-imidazol-1-ium; iodide. ^h Room temperature for 4 days. ⁱ 3-(1,3-Dihydro-isoindole-2-carbonyl)-1-methyl-3H-imidazol-1-ium; iodide. ^j 3-(2,3-Dihydro-indole-1-carbonyl)-1-methyl-3H-imidazol-1-ium; iodide. ^k 4-Morpholinecarbonyl chloride. ^l 3-(2,6-Dimethyl-morpholine-4-carbonyl)-1-methyl-3H-imidazol-1-ium; iodide. ^m IC₅₀ \pm SEM ($n = 5$). ⁿ 1-Methyl-3-(piperidine-1-carbonyl)-3H-imidazol-1-ium; iodide. ^o Room temperature for 2 days.

Results and Discussion

Optimization of HSL Inhibitors. A high-throughput screening was performed to identify HSL inhibitors. A range of inhibitors were identified and subjected to different counter screens, and compound **9a** was selected as one of the lead structures that should be investigated further. Compound **9a** is a potent HSL inhibitor with an IC₅₀ value of 350 nM. It is also a very weak inhibitor of butyrylcholine esterase (BChE), with an IC₅₀ value of 19 μ M. (The enzyme source is recombinant human enzyme.) We decided to prepare a few *N,N*-disubstituted carbamate analogues of compound **9a** as shown in Table 1. Only the *N*-methyl-*N*-phenyl carbamate analogue of compound **9d** had a reasonable HSL inhibition profile as it inhibited HSL with

an IC₅₀ value of 630 nM, and fortunately, did not inhibit BChE and acetylcholine esterase (AChE).

We synthesize a small range of *N*-methyl-*N*-phenyl carbamate analogues of **9a** as shown in Table 2. As can be seen, **10c**, the trisubstituted pyridine analogue, was a potent and selective inhibitor of HSL, with an IC₅₀ value of 350 nM. The disubstituted pyridine analogues **10d** and **10e** were even more interesting as they were both able to inhibit HSL with an IC₅₀ value of 46 nM. None of the compounds inhibited BChE and AChE to any measurable extent. As **10e** is at least 10 times more potent than **9d**, we also evaluated the rat PK profile of **10e** and, as can be seen from Table 6, the compound had a quite high clearance (CL) of 61 ng/mL/kg, a low peroral bioavailability (F_{po}) of 16%,

Table 4. Enzyme Activity and Selectivity for Substituted Methyl-phenyl Carbamate-Based HSL Inhibitors

No	Molecule	HSL IC ₅₀ (μM)	AChE IC ₅₀ (μM)	BChE IC ₅₀ (μM)	Preparation Method	Purification	Yield/%
10e		0.046 ± 0.019 ^a	>50	>50	-	-	-
12a		0.039	> 50	> 50	3 ^b	Prep. HPLC	76
12b		0.25	> 50	> 50	3 ^c	Prep. HPLC	76
12c		0.32	> 50	> 50	3 ^d	Prep. HPLC	79
12d		0.026 ± 0.005 ^e	> 50	> 50	3 ^f	Prep. HPLC	48
12e		0.071	> 50	> 50	3 ^g	Prep. HPLC	61
12f		1.5	>50	>50	2 ^h	Chromatography EtOAc/heptane (1:5) Reflux 18h	77
12g		0.051	> 50	> 50	3 ⁱ	Preparative HPLC	63
12h		0.023	> 50	> 50	3 ^j	Prep. HPLC	61

^a IC₅₀ ± SEM (*n* = 5). ^b (2-Methyl-phenyl)-methyl-amine. ^c (3-Methyl-phenyl)-methyl-amine. ^d (4-Methyl-phenyl)-methyl-amine. ^e IC₅₀ ± SEM (*n* = 2). ^f (2-Chloro-phenyl)-methyl-amine. ^g (3-Chloro-phenyl)-methyl-amine. ^h 3[(4-Chlorophenyl)-methyl-carbamoyl]-1-methyl-3*H*-imidazol-1-ium; iodide, reflux 18 h. ⁱ (2-Methoxy-phenyl)-methyl-amine. ^j (3-Methoxy-phenyl)-methyl-amine.

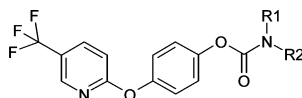
and a low maximum plasma concentration (*C*_{max}) of 43 ng/mL after a p.o. dose of 2.2 mg/kg and an i.v. dose of 11 mg/kg. It was decided to use the phenol part of **10e** in the search for other preferred amines other than the *N*-methyl-*N*-phenyl amine part of **9d**. First we investigated different *N*-methyl-*N*-alkyl amines (compound **11a–c**; Table 3). The isobutyl, *tert*-butyl, and cyclohexyl analogues were all weak inhibitors of HSL (IC₅₀ > 5 μM) despite having a bulky substituent at the methyl amine part of the carbamate. The *N*-methyl-*N*-benzyl **11d** (IC₅₀ = 1.4 μM) and *N*-ethyl-*N*-phenyl carbamate **11e** (IC₅₀ > 5 μM) were also not capable of inhibiting HSL to any degree of importance. As these five quite close structural analogues of **10e** are at least 50 times weaker inhibitors of HSL, it seems like the *N*-methyl-*N*-phenyl amine part of the carbamate is a preferred structural element.

We synthesize a range a cyclic amine based carbamates (entry **11f–11m**) and, as can be seen the pyrrolidine (**11f**), morpholine (**11i**), and piperidine (**11k**) carbamates, all are capable of inhibiting HSL with IC₅₀ values of 23, 250, and 65 nM, respectively. The annelated analogues **11g** and **11h** of **11f** were both not capable of inhibiting HSL to any degree of importance (IC₅₀ > 3 μM). The two annelated analogues **11i** (IC₅₀ = 1.1 μM) and **11m** (IC₅₀ > 5 μM) of **11k** were also quite weak inhibitors. These results demonstrate that the active site pocket corresponding to this position seems to be quite narrow.

As the *N*-methyl-*N*-phenyl-amine part of **10e** seems to be an important element, it was decided to synthesize a range of substituted phenyl analogues, as shown in Table 4. Compound

10e is quite a lipophilic compound with a PSA (polar surface area) value of 48.4 Å² and a cLogP value of 4.97 (Table 6). The analogues shown in Table 4 are even more lipophilic and probably unsuited as drug candidates, but the structure–activity relationship is very valuable as a starting point for the introduction of more hydrophilic structural elements in the phenyl part of the *N*-methyl-*N*-phenyl amine. A methyl group is well tolerated in both the ortho (**12a**), meta (**12b**), and para (**12c**) position, but the ortho methyl analogue **12a** is the most potent inhibitor with a IC₅₀ value of 39 nM (**12b**; IC₅₀ = 250 nM and **12c**; IC₅₀ = 320 nM). A more bulky and lipophilic chloro atom is well tolerated in the ortho (**12d**; IC₅₀ = 26 nM) and meta position (**12e**; IC₅₀ = 71 nM) but not in the para position (**12f**; IC₅₀ = 1.5 μM). Contrary to this, a methoxy group is well tolerated in both the ortho (**12g**; IC₅₀ = 51 nM) and para (**12h**; IC₅₀ = 23 nM) position. In conclusion, substituents are tolerated in all positions of the phenyl core.

As pyrrolidine- and piperidine-based cyclic amines are well tolerated, we prepare a range of substituted piperidine carbamates, as a large range of substituted piperidines are commercially available. To investigate if it was at all possible to find a position in the piperidine ring where a substitution is allowed, it was decided to synthesize and test the 2-, 3-, and 4-methyl-substituted analogues (compounds **13a–c**; Table 5). As can be seen, a methyl group is tolerated in the 4-position, as **13c** is a potent inhibitor of HSL, with an IC₅₀ value of 120 nM. Unfortunately, **13c** is also a weak inhibitor of BChE, with an IC₅₀ value of 16 μM. Furthermore, 4-substituted piperidin-

Table 5. Enzyme Activity and Selectivity for Substituted Piperidine Carbamate-Based HSL Inhibitors

No	Molecule	HSL IC ₅₀ (μM)	AChE IC ₅₀ (μM)	BChE IC ₅₀ (μM)	Preparation Method	Purification	Yield/%
11k		0.065 ± 0.016	>50	8.2	-	-	-
13a		>5	>50	> 50	2 ^{c,e}	Chromatography EtOAc/heptane (1:6)	71
13b		2.4	>50	>50	2 ^{c,f}	Chromatography EtOAc/heptane (1:6)	75
13c		0.12	>50	16	2 ^{c,g}	Chromatography EtOAc/heptane (1:6)	73
13d		1.1	>10	>50	3 ^h	Prep. HPLC	30
13e		0.21	>50	0.082	2 ^{c,i}	Chromatography EtOAc/heptane (1:6)	72
13f		0,11 ± 0.03	>50	>50	3 ^j	Recrystallized EtOAc/Heptane (1:2)	55
13g		0.50 ± 0.045	>50	>50	3 ^k	Chromatography EtOAc/heptane (1:1 →1:0)	73

^a Room temperature for 4 days. ^b 3-(3,4-Dihydro-1*H*-isoquinoline-2-carbonyl)-1-methyl-3*H*-imidazol-1-ium; iodide. ^c Reflux, 20 h. ^d 1-Methyl-3-(7-trifluoromethyl-3,4-dihydro-2*H*-quinoline-1-carbonyl)-3*H*-imidazol-1-ium; iodide. ^e 1-Methyl-3-(2-methyl-piperidine-1-carbonyl)-3*H*-imidazol-1-ium; iodide. ^f 1-Methyl-3-(3-methyl-piperidine-1-carbonyl)-3*H*-imidazol-1-ium; iodide. ^g 1-Methyl-3-(4-methyl-piperidine-1-carbonyl)-3*H*-imidazol-1-ium; iodide. ^h Phenyl-piperidin-4-yl-methanone. ⁱ 3-(4-Benzyl-piperidine-1-carbonyl)-1-methyl-3*H*-imidazol-1-ium; iodide. ^j Piperidin-4-yl-methanol. ^k 4-Piperidinol.

Table 6. Comparison of Calculated Properties and PK Properties for Selected HSL Inhibitors

No	ClogP	PSA (Å ²)	C _{max} (ng/mL)	CL (mL/min/kg)	F _{po} (%)	% reduction of glycerol (p.o.)	exp (ng/mL)
10e	4.97	48.4	43 ^a	61 ^a	16 ^a		
11i	2.98	61.3	21 ^b	203 ^b	12 ^b		
13f	2.78	75.4	60 ^a	46 ^a	10 ^a	59 ^d	379 ^d
13g	2.16	75.6	1220 ^c	9 ^c	56 ^c	42 ^d	3202 ^d

^a Tested at 1.1 mg/kg (i.v.) and 2.2 mg/kg (p.o.). ^b Tested at 0.5 mg/kg (i.v.) and 1.0 mg/kg (p.o.). ^c Tested at 1.2 mg/kg (i.v.) and 2.4 mg/kg (p.o.). ^d 10 mg/kg p.o., *n* = 4.

carbamates were synthesized (compound **13d–g**; Table 5). The 4-carboxy-phenyl analogue **13d** was only a very weak inhibitor of HSL, but the 4-benzyl (**13e**; IC₅₀ = 210 nM), 4-hydroxymethyl (**13f**; IC₅₀ = 110 nM), and 4-hydroxy (**13g**; IC₅₀ = 450 nM) were all potent inhibitors of HSL. Unfortunately, the 4-benzyl analogue was also a potent inhibitor of BChE. Nevertheless, the results demonstrate that large substituents are well tolerated in the 4-position of the piperidine part of compound **11k**. Fortunately, the introduction of a hydroxyl group as in **13f** and **13g** is not tolerated for inhibition of BChE and AChE, making the two compounds selective.

As demonstrated by Wei³¹ and Yeh,³² the introduction of a polar group in a lipophilic saturated ring system can in some cases greatly improve the PK profile compared to the more lipophilic nonsubstituted analogue (properties for the PK preferred structure RPR 127963: ClogP, 2.47 and PSA, 88 Å²). For lipophilic parts of molecules, it is expected that the introduction of polar groups in some cases make saturated ring systems less susceptible for CYP 3A4 derived degradation. The overall properties for the respective compound is, of course,

also of great importance. The introduction of polar groups will in general increase PSA and decrease clogP.

Compounds **11i**, **13f**, and **13g** are selective and potent inhibitors of HSL and they all contain solubilizing hydroxyl groups or ether groups that have a positive influence on the hydrophilicity (increased solubility). The PSA level is increased to about 61 Å² for **11i** and to 75 Å² for **13f** and **13g** and the clogP value is reduced to 2–3 compared to the PSA of 48 Å² and clogP of 4.97 for **10e**. The PK profile of **13f** and **13g**, which have clogP and PSA properties close to the properties of RPM 127963, were evaluated further together with **11i** (Figure 3).

The PK profile for the three compounds were measured (Figure 3 and Table 6) and it was found that **11i** had a very high CL of 203 mg/min/kg, a low F_{po} of 12%, and a low C_{max} of 21 ng/mL after an intravenous (i.v.) dose of 1.1 mg/kg and a per oral (p.o.) dose of 2.2 mg/kg, which disqualified the compound for further investigations. Compound **13f** had a high CL of 46 mg/min/kg, a low C_{max} of 60 ng/mL and a low F_{po} of 10 mg/kg after an i.v. dose of 0.5 mg/kg and a p.o. dose of 1.0 mg/kg. In contrast to these two compounds, **13g** has a much more promising PK profile with a CL of 9 mg/min/kg, a C_{max} of 1220 ng/mL, and a F_{po} of 56% (i.v. dose of 1.2 mg/kg and p.o. dose of 2.4 mg/kg). The promising PK profile seen for **13g** further support the hypothesis that introduction of polar groups in saturated rings can greatly improve the PK profiles of compounds. The challenge is to find positions where polar groups also are tolerated potency vice. Both compounds **13f** and **13g** were evaluated in an acute in vivo rat PK/PD model at 10 mg/kg and plasma glycerol was measured as lipolytic endpoint. As can be seen from Table 6 and Figure 4, both compounds were capable of significantly reducing the plasma glycerol levels acutely. This correlates well with the in vivo

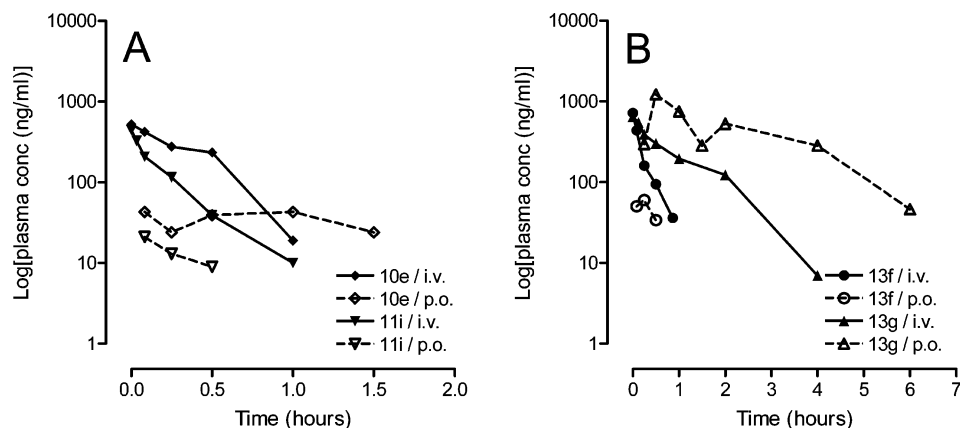


Figure 3. PK profiles for selected carbamate-based HSL inhibitors. A, **10e** and **11i**; and B, **13f** and **13g**.

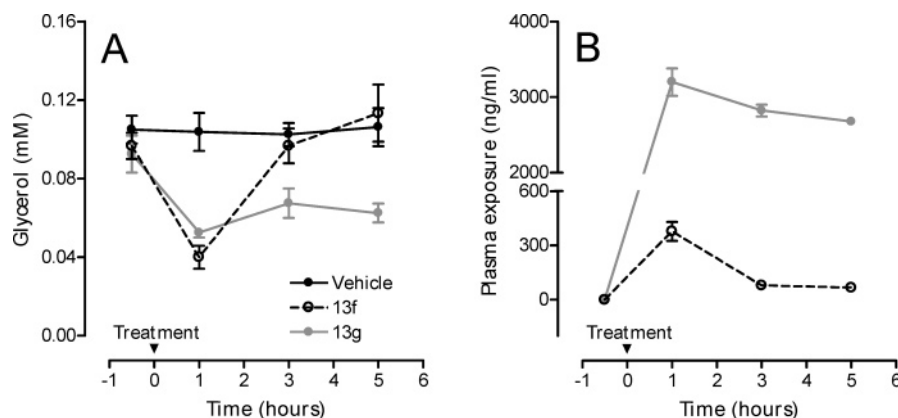


Figure 4. PK/PD profile (10 mg/kg) for **13f** and **13g**.

data published by Claus³³ for **1**. In line with the PK profile for the two compounds, **13g** has a longer duration of action. The maximum exposure levels after 1 h were 379 ng/mL and 3202 ng/mL for **13f** and **13g**, respectively. Compounds **13f** and **13g** did not inhibit the 3 CYP isoforms 1A2, 2C9, and 2D6 and were also not capable of inhibiting PL, LPL, and HL.

Conclusion

We have identified a novel type of carbamate-based HSL inhibitors. It is expected that the compounds are reversible pseudo-substrate inhibitors like a range of other known HSL inhibitors. Compounds within different classes of carbamate-based HSL inhibitors are potent and selective and all compounds have full efficacy. The *N*-methyl-*N*-phenyl carbamates are in general the most potent inhibitors of HSL, with IC₅₀ values for a range of compounds below 50 nM.

The two piperidine carbamate based HSL inhibitors **13f** and **13g** were potent and selective HSL inhibitors, with IC₅₀ values of 110 and 450 nM, respectively. As both compounds have a promising PK profile and increased solubility due to the influence of the hydroxy groups, they were tested in an acute PK/PD study in rats. Both compounds showed acute antilipolytic activity at a dose of 10 mg/kg p.o., did not inhibit the 3 CYP isoforms 1A2, 2C9 and 2D6 and were not capable of inhibiting any other lipase or esterase tested (HL, PL, LPL, BChL and AChL). Due to the promising profile seen for **13f** and **13g** further studies will be conducted to evaluate the biological importance of inhibiting HSL.

Experimental Section

Materials and Methods. NMR data were recorded on a 300 MHz and on a 400 MHz spectrometer. Assignments: quint, quintet; sext, sextet. Elemental analyses were within 0.4% of the calculated

values. Human recombinant HSL was prepared as described by Holm et al.³⁴ Human hepatic lipase and bovine lipoprotein lipase³⁵ were kindly provided by Professor Gunilla Olivecrona, Umeå University, Sweden. Apo CII was prepared as described by Holm et al.³⁶

Butyl-carbamic acid (4-(3,5-dichloropyridin-2-yloxy)-phenyl ester was purchased from Specs. The respective 1-methyl-3*H*-imidazol-1-ium iodides were prepared as described by Batey et al.³⁷ Chloroformates were synthesized from the appropriate phenols and phosgene or a phosgene substitute like, for example, trichloromethyl chloroformate, as described in Konakahara et al.,³⁸ except that the crude product was separated from the diisopropylethylamine hydrochloride by extraction with diethyl ether rather than with THF. 2-(4-Hydroxyphenoxy)-5-trifluoromethylpyridine was prepared as described by Watson and Serban.³⁹

HPLC-MS was measured on a Hewlett-Packard series 1100. Column: Waters X-terra MS C-18 × 3 mm id. Gradient: 10–100% acetonitrile (0.01% TFA) linear during 7.5 min at 1.0 mL/min. Detection: 210 nm (analogue output from DAD). MS: ionization mode API-ES, scan 100–1000 amu step 0.1 amu.

Preparative HPLC. The system consists of two Gilson 322 pumps and a Gilson manometric module 805. A Gilson 215 combined auto-injector and fraction collector performs injection and fraction collection. Detection is performed with a Gilson Diode array detector 170. A sample containing 25–100 mg of material dissolved in 0.5–2.0 mL of solvent (minimum water concentration: 10%).

Separation is performed on Waters Xterra, RP₁₈ 7 μm, columns 19 mm × 150 mm, flow rate 15 mL/min (sample added with a flow rate of 5 mL/min for about 1 min). The most widely used gradient starts at 5% acetonitrile in water and ends after 14 min on 95% acetonitrile. This concentration is maintained for 6 min. The system is buffered with 0.05% TFA. In special cases, the gradient is altered to fit the separation need. The pooled fractions are evaporated to dryness in vacuo.

The inhibition of the different lipases and esterases (HSL, HL, LPL, PL, AChE, and BChE) were determined as described in Ebdrup et al.²⁹ The lipase assays were based on a new fluorochrome-labeled triacylglyceride octadec-9-enoic acid 2-[12-(7-nitrobenzo^{1,2,5}oxadiazol-4-ylamino)-dodecanoyloxy]-1-octadec-9-enoyloxymethyl-ethyl ester, and the AChE and BChE assays were based on acetylthiocholine or butyrylthiocholine, respectively. Maximum concentration of inhibitors for determination of IC₅₀ values was 100 μ M, with 5-fold dilution steps in six concentrations. Each data point was determined as the average of two measurements. IC₅₀ values were calculated using Prism, version 4.0, by fitting the data to a sigmoidal dose-response (variable slope) nonlinear regression analyses.

General Procedure 1. The appropriate phenol was dissolved in dry THF (30 mL) and 1,4-diazadicyclo[2.2.2]octane (0.89 g, 8.0 mmol) and a carbamoyl chloride (6.0 mol) was added, and the reaction mixture was stirred overnight at room temperature. A 3% aqueous citric acid solution (30 mL) was added and the phases were separated. The aqueous phase was extracted with dichloromethane (30 mL \times 3) and the pooled organic phases were dried and evaporated to dryness to give the crude product.

General Procedure 2. The phenol (2.0 mmol) was dissolved in acetonitrile (30 mL) in a glass screw cap vessel. Triethylamine (2.0 mmol) was added together with the respective 1-methyl-3*H*-imidazol-1-ium iodide (2.0 mmol) dissolved in acetonitrile (30 mL) at room temperature. The reaction mixture was shaken for 16–48 h at reflux and evaporated. Dichloromethane (30 mL) and 0.1 N aqueous hydrochloric acid solution (20 mL) was added, the organic phase was separated, and the aqueous phase was extracted with dichloromethane (2 \times 30 mL). The combined organic phases were washed with water (10 mL), dried, and evaporated to give the crude product.

General Procedure 3. The appropriate aryl chloroformate (4.0 mmol) was dissolved in dry THF or dichloromethane (30 mL). An appropriate amine (6.0 mmol) and diisopropylethylamine (0.105 g, 6.0 mmol) were added, and the reaction mixture was stirred overnight at room temperature. The crude reaction mixture was evaporated to dryness to give the crude product.

The preparative and purification methods used and the yields obtained are described in Tables 1–5 for each individual compound. The Spectroscopic data, LC-MS and elemental analyses can be found in the Supporting Information.

4-Hydroxymethyl-piperidine-1-carboxylic Acid 4-(5-Trifluoromethylpyridin-2-yloxy)-phenyl Ester, 13f. ¹H NMR (400 MHz, CDCl₃) δ 1.20–1.35 (m, 2H), 1.68–1.78 (m, 1H), 1.71 (br s, 1H), 1.78–1.86 (m, 2H), 2.86 (t, *J* = 12.1, 1H), 2.99 (t, *J* = 12.1, 1H), 3.54 (d, *J* = 6.0, 2H), 4.32 (t, *J* = 14, 2H), 7.00 (d, *J* = 8.6, 1H), 7.11–7.19 (m, 4H), 7.89 (dd, *J* = 8.5 and 2.5, 1H), 8.43 (m, 1H). ¹³C NMR (100 MHz, CDCl₃) δ 28.34 and 28.77 (ratio 1:1), 38.56, 44.19 and 44.49 (ratio 1:1), 67.31, 111.13, 121.56 (q, *J* = 33.7 Hz), 122.23, 122.94, 123.65 (q, *J* = 271.5 Hz), 136.67 (q, *J* = 2.9 Hz), 145.44 (q, *J* = 4.4), 148.66, 150.03, 153.53, 165.79. LC-MS *R*_t 3.87 min, *m/z*: 397 (M + H)⁺, >99%. Anal. (C₁₉H₁₉F₃N₂O₄) C, H, N.

4-Hydroxy-piperidine-1-carboxylic Acid 4-(5-Trifluoromethylpyridin-2-yloxy)-phenyl Ester, 13g. ¹H NMR (CDCl₃) 1.54–1.66 (m, 2H), 1.73 (br s, 1H, minor), 1.79 (br s, 1H, major), 1.90–1.99 (m, 2H), 3.26 (t, *J* = 9, 1H), 3.37 (t, *J* = 9, 1H), 3.90–4.07 (m, 3H), 7.00 (d, *J* = 8.6, 1H), 7.11–7.21 (m, 4H), 7.89 (dd, *J* = 8.5 and 2.5, 1H), 8.42–8.46 (m, 1H). ¹³C NMR (100 MHz, CDCl₃) δ 33.90 (d, *J* = 26.3), 41.65 (d, *J* = 21.2), 66.97, 111.15, 121.59 (q, *J* = 33), 122.16, 122.94, 123.62 (q, *J* = 271.5), 136.73 (q, *J* = 3), 145.38 (q, *J* = 4), 148.57, 150.05, 153.53, 165.74. LC-MS *R*_t 3.63 min, *m/z*: 383 (M + H)⁺, >98%. Anal. (C₁₈H₁₇F₃N₂O₄) C, H, N.

Pharmacokinetic Studies in Rat. The p.o. dose was around 2 mg/kg and the i.v. dose was around 1 mg/kg, and the dosing solution contained 10% hydroxy propyl cyclodextrin (HPCD) in phosphate buffer pH 7.0. However, **11i** was dosed with 20% tween 80 and 5% glucose in phosphate buffer, pH 7.0. The compounds were dosed p.o. by gavage and i.v. in the tail vein to male Sprague–

Dawley rats (Charles River Sulzfeld, Germany). Blood samples were collected by heart puncture under carbon dioxide anaesthesia in ethylene diamine tetraacetic acid EDTA–NaF tubes at predetermined time points. A rat was applied for each time point.

PK/PD Studies in Rats. Animals: Male Sprague–Dawley rats, twelve weeks of age, were purchased from Charles River (Sulzfeld, Germany). The rats were housed under constant humidity in a temperature- (20 \pm 2 $^{\circ}$ C) and light-controlled environment (12 h light/dark cycle; lights on from 6 a.m.), with free access to food (Altromin 1324) and water. All experimental procedures were approved by the Danish Animal Experiment Inspectorate.

In Vivo Inhibition of Lipolysis. The acute effects of HSL inhibition were tested in vivo in the overnight fasted rats using plasma glycerol as antilipolytic biomarker. Briefly, overnight fasted rats received vehicle (*n* = 8 or HSL inhibitor (10 mg/kg body weight p.o.; *n* = 4 per group). Blood samples were collected at baseline (0.5 h before dosing of compound) and again 1, 3, and 5 h after dosing of compound. Blood was drawn from orbital plexus (anaesthetic: isofluran, Abbott Scandinavia AB, Sweden) into EDTA-coated tubes containing 0.1% NaF (W/V) and was plasma collected. Plasma samples were stored at –80 $^{\circ}$ C before analysis. Plasma glycerol levels were determined using standard laboratory procedures (Hitachi 912 automatic analyzer, Boehringer Mannheim).

Plasma Analysis. Plasma samples were analyzed by turbulent flow chromatography combined with tandem mass spectrometry (TFC–MS/MS). Plasma sample preparation included dilution (10% methanol, 1:1), centrifugation (14 300 g for 20 min), and aliquotation of a minimum of 100 μ L to 96-well plates. TFC was performed using a 2300 HTLC system (Cohesive Technologies) consisting of an isocratic pump for sample cleanup and flush of liquid lines, a binary pump for elution of retained analytes, and a valve switching module with two Rheodyne six-port valves. The autosampler was a CTC HTS PAL (CTC Analytics, Zingen, Switzerland). Injection volumes were 50 μ L. A single column method with a Waters Oasis HLB, 1.0 \times 50 mm, column was used, except for **11i**, where a Cohesive Turbo column, C8 50 μ m, was applied. The mobile phases were A, methanol–0.1% formic acid (5:95, v/v), and B, methanol–0.1% formic acid (95:5, v/v), except for **10e**, where mobile phase A, 0.05% trifluoroacetic acid, and mobile phase B, 0.05% trifluoroacetic acid in acetonitrile, were used. Samples containing the compounds were extracted from the plasma and eluted into the interface on the mass spectrometer, using the following three-step method: step 1, the sample was loaded onto the column with an aqueous mobile phase (100% A); step 2, elution of analytes to detector with mobile phase B; and step 3, system re-equilibration.

Samples were analyzed by MS–MS using a MDS Sciex API 3000 triple quadrupole tandem mass spectrometer (Toronto, Canada) equipped with a Turbo Ion Spray interface. The mass spectrometer was operated in positive-ion multiple reaction monitoring (MRM) mode with key parameter settings: temperature, 350; ionization current, 4500–5000; orifice potential, 25–70; and ring potential, 100–360. The molecular ions and production ions for the individual compounds were **13f**, 397.1 \rightarrow 142.0; **10e**, 389.1 \rightarrow 134.0; **11i**, 369.2 \rightarrow 114.3; and **13g**, 383.1 \rightarrow 127.9. Calibration curves were prepared for each compound dissolved in plasma in the concentration range 10–3000 ng/mL.

CYP Inhibition Assay. The in vitro CYP-subtype activity in the absence and presence of a test compound (the potential CYP-subtype inhibitor) was determined using a CYP-subtype selective substrate (dextromethorphan for CYP2D6, erythromycin for CYP3A4, and phenacetin for CYP1A2, respectively). Incubations were utilized (200 μ L, 37 $^{\circ}$ C, 10 min) containing human liver microsomes (HLM, 0.1 mg), [*O*-methyl-¹⁴C]-dextromethorphan in the CYP2D6 assay (total concn: 3 μ M = *K*_m), [*N*-methyl-¹⁴C]erythromycin and erythromycin in the CYP3A4 assay (total concn: 20 μ M = *K*_m), or [*O*-ethyl-¹⁴C]phenacetin and phenacetin in the CYP1A2 assay (total concn: 40 μ M = *K*_m), the cofactor NADPH (1 mM), and the test compound (20 μ M). All incubations were performed in triplicate. The HLM preparations used were a pool of \geq 15 donors to obtain

an average concentration of CYP subtypes, which is known to differ markedly between individuals.

The metabolic conversion of [*O*-methyl-¹⁴C]-dextromethorphan, [*N*-methyl-¹⁴C]erythromycin, or [*O*-ethyl-¹⁴C]phenacetin, respectively, were assessed by activated charcoal extraction, followed by liquid scintillation counting of the supernatant. The thereby measured ¹⁴C-formaldehyde reflected the metabolism of the selective substrate by CYP subtype.

Acknowledgment. The technical assistance from Aase Vinterby, Johnny Madsen, Lotte Gottlieb Sørensen, Helle Bach, and Freddy Z. Pedersen are highly appreciated.

Supporting Information Available: Spectroscopic data, LC-MS, and elemental analyses are available free of charge via the Internet at <http://pubs.acs.org>.

References

- DeFronzo, R. A. Pathogenesis of type 2 (non-insulin dependent) diabetes mellitus: A balanced overview. *Diabetologia* **1992**, *35*, 389–397.
- Unger, R. H. Lipotoxic diseases. *Ann. Rev. Med.* **2002**, *53*, 319–336.
- Rossetti, L.; Giaccari, A.; DeFronzo, R. A. Glucose toxicity. *Diabetes Care* **1990**, *13*, 610–630.
- McGarry, J. D. Dysregulation of fatty acid metabolism in the etiology of type 2 diabetes. *Diabetes* **2002**, *51*, 17–18.
- Reaven, G. M.; Greenfield, M. S. Diabetic hypertriglyceridemia: Evidence for three clinical syndromes. *Diabetes* **1981**, *30*, 66–75.
- Frayn, K. N. Adipose tissue as a buffer for daily lipid flux. *Diabetologia* **2002**, *45*, 1201–1210.
- Unger, P. H. Lipotoxicity in the pathogenesis of obesity-dependent NIDDM. Genetic and clinical implications. *Diabetes* **1995**, *44*, 863–870.
- Boden, G. Role of fatty acids in the pathogenesis of insulin resistance and NIDDM. *Diabetes* **1997**, *46*, 3–10.
- Boden, G.; Jadali, F.; White, J.; Liang, Y.; Mozolli, M.; Chen, X.; Coleman, E.; Smith, C. Effects of fat on insulin stimulated carbohydrate metabolism in normal men. *J. Clin. Invest.* **1991**, *88*, 960–966.
- Kim, J. K.; Fillmore, J. J.; Chen, Y.; Yu, C.; Moore, I. K.; Pypaert, M.; Lutz, E. P.; Kako, Y.; Velez-Carrasco, W.; Goldberg, I. J.; Breslow, J.; Schulman, G. I. Tissue-specific overexpression of lipoprotein lipase causes tissue-specific insulin resistance. *Proc. Natl. Acad. Sci. U.S.A.* **2001**, *98*, 7522–7527.
- Ferranini, E.; Barret, E. J.; Bevilacqua, S.; DeFronzo, R. A. Effect of fatty acids on glucose production and utilization in man. *J. Clin. Invest.* **1983**, *72*, 1737–1747.
- Boden, G.; Jadali, F. Effects of lipid on basal carbohydrate metabolism in normal men. *Diabetes* **1991**, *40*, 686–692.
- Large, V.; Arner, P. Regulation of lipolysis in humans. Pathophysiological modulation in obesity, diabetes and hyperlipidemia. *Diabetes Metab.* **1998**, *24*, 409–418.
- Groop, L. C.; Saloranta, C.; Shank, M.; Bonadonna, R. C.; Ferrannini, E.; DeFronzo, R. A. The role of free fatty acid metabolism in the pathogenesis of insulin resistance in obesity and noninsulin-dependent diabetes mellitus. *J. Clin. Endocrinol. Metab.* **1991**, *72*, 96–107.
- Ginsberg, H.; Plutzky, J.; Sobel, E. Review of metabolic and cardiovascular effects of oral antidiabetic agents: Beyond glucose-level lowering. *J. Cardiovasc. Risk* **1999**, *6*, 337–346.
- Miles, J. M.; Wooldridge, D.; Grellner, W. J.; Windsor, S.; Isley, W. L.; Kelin, S.; Harris, W. S. Nocturnal and postprandial free fatty acid kinetics in normal and type 2 diabetic subjects. *Diabetes* **2003**, *52*, 675–681.
- Coppack, S. W.; Evans, R. D.; Fischer, R. M.; Frayn, K. N.; Gibbons, G. F.; Humphreys, S. M.; Kirk, M. L.; Potts, J. L.; Hockaday, T. D. Adipose tissue metabolism in obesity: Lipase action in vivo before and after a mixed meal. *Metabolism* **1992**, *41*, 264–272.
- Kraemer, F. B.; Shen, W.-J. Hormone sensitive lipase: Control of intracellular tri-(di)-acylglycerol and cholesteryl ester hydrolyses. *J. Lipid. Res.* **2002**, *43*, 1585–1594.
- Langin, D.; Holm, C.; LaFontan, M. Adipocyte hormone sensitive lipase: a major regulator of lipid metabolism. *Proc. Nutr. Soc.* **1996**, *55*, 93–109.
- Wang, S. P.; Laurin, N.; Himms-Hagen, J.; Rudnicki, M. A.; Levy, E.; Robert, M.-F.; Pan, L.; Oligny, J.; Mitchell, G. A. A. The adipose tissue phenotype of hormone-sensitive lipase deficiency in mice. *Obes. Res.* **2001**, *9*, 119–128.
- Okazaki, H.; Osuga, J.-I.; Tamura, Y.; Yahagi, N.; Tomita, S.; Shionoiri, F.; Iizuka, Y.; Ohashi, K.; Harada, K.; Kimura, S.; Gotoda, T.; Shimano, H.; Yamada, N.; Ishibashi, S. Lipolysis in the absence of hormone-sensitive lipase: Evidence for a common mechanism regulating distinct lipases. *Diabetes* **2002**, *51*, 3368–3375.
- Haemmerle, G.; Zimmermann, R.; Hayn, M.; Theussl, C.; Waeg, G.; Wagner, E.; Sattler, W.; Magin, T. M.; Wagner, E. F.; Zechner, R. Hormone-sensitive lipase deficiency in mice causes diglyceride accumulation in adipose tissue, muscle, and testis. *J. Biol. Chem.* **2002**, *277*, 4806–4815.
- Zimmermann, R.; Strauss, J. G.; Haemmerle, G.; Schoiswohl, G.; Birner-Gruenberger, R.; Riederer, M.; Lass, A.; Neuberger, G.; Eisenhaber, F.; Hermetter, A.; Zechner, R. Fat mobilisation in adipose tissue is promoted by adipose triglyceride lipase. *Science* **2004**, *306*, 1383–1386.
- Lowe, D. B. In vitro SAR of (5-2H)-isoxazolonylureas, potent inhibitors of hormone-sensitive lipase. *Bioorg. Med. Chem. Lett.* **2004**, *14*, 3155–3159.
- Shoenfinger, K.; Petry, S.; Mueller, G.; Barringhaus, K.-H. PCT Appl. WO 0166533, 2001.
- Petry, S.; Schoenfinger, K.; Mueller, G.; Barringhaus, K.-H. PCT Appl. WO 0117981, 2001.
- Slee, D. H.; Bhat, A. S.; Nguyen, T. N.; Kish, M.; Lundeen, K.; Newman, M. J.; McConnell, S. J. Pyrrolopyrazinedione-based inhibitors of hormone-sensitive lipase. *J. Med. Chem.* **2003**, *46*, 1120–1122.
- C. de Jong, J.; Sørensen, L. G.; Tornqvist, H.; Jacobsen, P. Carbazates as potent inhibitors of hormone-sensitive lipase. *Bioorg. Med. Chem. Lett.* **2004**, *14*, 1741.
- Ebdrup, S.; Sørensbek, L. G.; Olsen, O. H.; Jacobsen, P. Synthesis and structure–activity relationship for a novel class of potent and selective carbamoyl-triazole based inhibitors of hormone sensitive lipase. *J. Med. Chem.* **2004**, *47*, 400–410.
- Ebdrup, S.; Jacobsen, P.; Dhanda Farrington, A.; Vedsø, P. Structure–activity relationship for aryl and heteroaryl boronic acid inhibitors of hormone-sensitive lipase. *Bioorg. Med. Chem.* **2005**, *13*, 2305–2312.
- Wei, H.; Myers, R.; Hanney, B.; Spada, A. P.; Bilder, G.; Galzinski, H.; Amin, D.; Needle, S.; Page, K.; Jazosi, Z.; Perrone, M. H. Potent quinoxaline-based inhibitors of PDGF receptor tyrosin kinase activity. Part 2: The synthesis and biological activities of RPR127963, an orally bioavailable inhibitor. *Bioorg. Med. Chem. Lett.* **2003**, *13*, 3097–3100.
- Yeh, S. C.; Patel, J. R.; Kurukulasuriya, H. Y. R.; Fung, S.; Monzon, K.; Chiou, W.; Wang, J.; Stolarik, D.; Imade, H.; Beno, D.; Brune, M.; Jacobsen, P.; Sham, H.; Link, J. T. Synthesis and biological evaluation of heterocyclic containing adamantane 11 β -HSD1 inhibitors. *Bioorg. Med. Chem. Lett.* **2006**, *16*, 5414–5419.
- Claus, T. C.; Lowe, D. B.; Liang, Y.; Salhanick, A. I.; Lubeski, C. K.; Yang, L.; Lemoine, L.; Zhu, J.; Clairmont, A. I. Specific inhibition of hormone-sensitive lipase improves lipid profiles with reducing plasma glucose. *J. Pharmacol. Exp. Ther.* **2005**, *315*, 1396–1402.
- Contreras, J. A.; Danielsson, B.; Johansson, C.; Osterlund, T.; Langin, D.; Holm, C. Human hormone sensitive lipase—Expression and large-scale purification from a baculovirus/insect cell system. *Protein Expression Purif.* **1998**, *12*, 93–99.
- Bengtson-Olivecrona, G.; Olivecrona, T. Phospholipase activity of milk lipoprotein lipase. *Methods Enzymol.* **1991**, *197*, 345–356.
- Holm, C.; Olivecrona, G.; Ottoson, M. Assays of lipolytic enzymes. *Methods Mol. Biol.* **2001**, *155*, 97–119.
- Batey, R. A.; Santhakumar, V.; Yoshina-Ishii, C.; Tayler, S. D. An efficient new protocol for the formation of unsymmetrical tri- and tetrasubstituted ureas. *Tetrahedron Lett.* **1998**, *39*, 6267–6270.
- Konakahara, T.; Ozaki, T.; Sato, K.; Gold, B. A Convenient method for the synthesis of activated *N*-methylcarbamates. *Synthesis* **1993**, *1*, 103–106.
- Watson, K. G.; Serban, A. Evaluation of the elbs persulfate oxidation reaction for the preparation of aryloxyphenoxypropionate herbicides. *Aust. J. Chem.* **1995**, *48*, 8, 1503–1510.

JM0607653